Hydrodynamic Analysis of a Semi-Submersible-Type Floating Wind Turbine

Hu, Changhong
Research Institute for Applied Mechanics (RIAM), Kyushu University

Sueyoshi, Makoto
Research Institute for Applied Mechanics (RIAM), Kyushu University

Liu, Cheng
Interdisciplinary Graduate School of Engineering Science, Kyushu University

Liu, Yingyi
Interdisciplinary Graduate School of Engineering Science, Kyushu University

出版情報：Journal of Ocean and Wind Energy. 1 (4), pp.202-208, 2014-11. The International Society of Offshore and Polar Engineers
バージョン：

Journal of Ocean and Wind Energy (ISSN 2310-3604)

Vol. 1, No. 4, November 2014, pp. 202–208

http://www.isope.org/publications

Hydrodynamic Analysis of a Semi-Submersible-Type Floating Wind Turbine

Changhong Hu and Makoto Sueyoshi
Research Institute for Applied Mechanics (RIAM), Kyushu University
Kasuga, Fukuoka, Japan

Cheng Liu and Yingyi Liu
Interdisciplinary Graduate School of Engineering Science, Kyushu University
Kasuga, Fukuoka, Japan

A hydrodynamic analysis of a moored semi-submersible type floating wind platform has been carried out. Three methods are used in this study. The first method is the physical experiment that is carried out in the towing tank at the Research Institute for Applied Mechanics (RIAM), in which a movable seafloor frame to fix mooring lines and a wind generator are newly installed. The second method is the Computational Fluid Dynamics (CFD) simulation using our in-house research code RIAM-CMEN, which is used to predict strongly nonlinear wave and wind loads on the floating body in rough sea conditions. The third method is the potential flow-based numerical model, which is used as a practical analysis tool for parametric study. In this paper, the three methods are described and the accuracy of the two numerical methods to predict wave-body interactions is checked by comparison with the experiment.

INTRODUCTION

In recent years, several floating offshore wind farm projects have been planned in Japan. Severe ocean environmental conditions, such as typhoons, must be considered in the safety assessment. Due to strict cost-effective requirements for renewable energy development, conventional ocean platform technologies that have been developed and utilized in the offshore oil and gas (O&G) industries may not be directly applied to the design of an offshore wind platform. Such an economic restriction brings new technological challenges, and considerable research is required.

At Kyushu University, a research project is being carried out on the development of a semi-submersible-type floating wind turbine system. The system consists of a triangular-shaped platform with a large deck space, three diffuser-augmented wind turbines (the so-called Wind Lens turbines) installed on the columns, and solar panels installed on the deck. The platform is a composition of cylindrical structures, which can be constructed at a competitive cost. Since the offshore wind turbine system is planned to be operated in the sea areas with the depth below 100 meters, a catenary mooring system is used. Figure 1 is a computer graphic (CG) to show the conceptual design of the floating wind turbine. The development of a low-cost floating platform is one of the most important issues in this project. The wave response properties and the maximum wave and wind loads on the platform should be evaluated as accurately as possible to reduce the total weight of the platform and to satisfy the safety requirements. The existing experimental and numerical tools should be improved and combined for this purpose.

The final goal of this research is to develop an integrated analysis tool, which includes both a Computational Fluid Dynamics (CFD) code and a potential flow code for the optimization design and safety evaluation of the semi-submersible-type offshore wind turbine. The CFD code is an in-house research code (RIAM-CMEN), which is used to predict extremely nonlinear wave-body interactions and maximum wave and wind loads in harsh sea conditions. The basic numerical scheme adopted by the code is the Constrained Interpolation Profile (CIP)-based multi-phase simulation method. The computation domain covers water and air, with the free surface considered as an inner interface. This code has been developed to predict strongly nonlinear seakeeping problems (Hu and Kashiwagi, 2004; Hu et al., 2012). Extension of the code for the numerical simulation of a floating wind turbine by adding a wind turbine calculation module and a mooring line calculation module has also been carried out recently. The potential flow code is used as a practical analysis tool for the parametric study of the dynamic response of the platform in waves. The potential flow code development emphasizes the treatment of the nonlinear effects due to the aerodynamic loads on the Wind Lens turbine and the treatment of the dynamic loads due to the mooring lines.

In this paper, the recent progress of the research is reported. First, an experimental method using the towing tank for testing the floating wind turbine under large wave and strong wind conditions is presented. Then two numerical methods, the CFD method and the potential flow method, are described. Finally, some selected numerical cases on wave-body interaction are presented in comparison with the experiment.

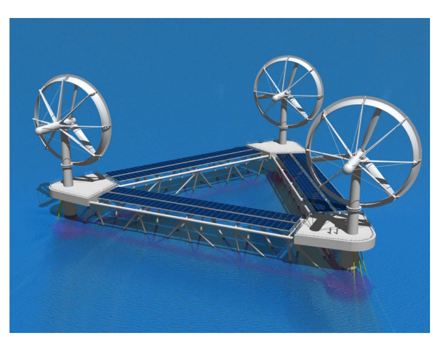

Fig. 1 An image of Kyushu University's floating wind turbine

Received May 22, 2014; revised manuscript received by the editors September 28, 2014. The original version was submitted directly to the Journal.

KEY WORDS: Floating offshore wind turbine, hydrodynamic analysis, CFD, potential flow method, model experiment.

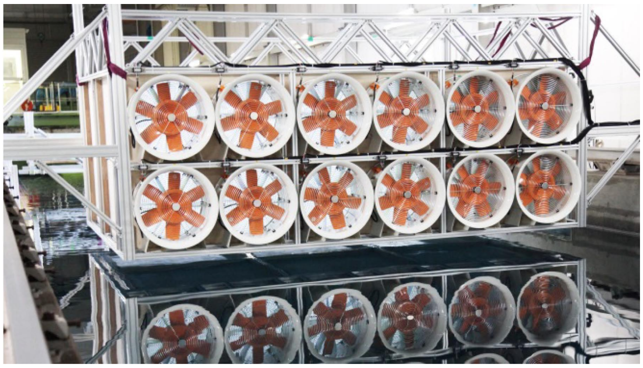

Fig. 2 Wind generator installed on the wave tank

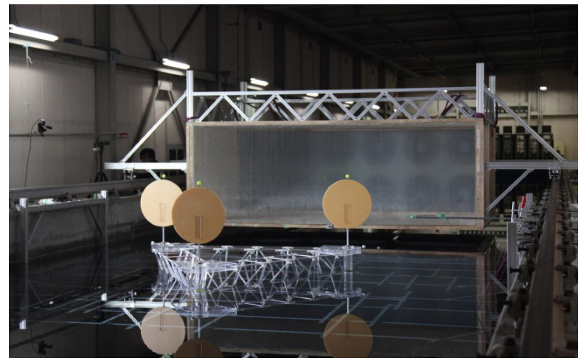

Fig. 3 A platform model with drag plates in the experiment

MODEL EXPERIMENT

The model experiment is carried out in the towing tank (65 m long, 5 m wide, and 7 m deep) at the Research Institute for Applied Mechanics (RIAM). The purpose of the experiment is to check the hydrodynamic performance of the platform and to provide a benchmark database for validation of the numerical simulation tools. Due to the limitation of the tank width, the mooring lines are approximated by a set of wires and springs. To simulate strong wind conditions, a wind generator is installed on the tank, as shown in Fig. 2. The wind generator is composed of 12 axial flow fans and is able to generate a maximum average wind speed of 5 m/s at the location of 3 m downstream.

Preliminary numerical studies of this platform indicate that the drift force and the motion amplitudes caused by the incident waves are small in the operational sea state condition. Therefore, a simple linear spring system is used in the experiment to approximate the anchor-chain mooring system. The mooring lines are connected to the corners of the triangular-shaped platform. To satisfy the water depth requirement, a movable seafloor frame is installed on the towing tank, and the mooring lines are connected to the anchoring point on the frame. Load cells are equipped at the end of each spring to detect the mooring line tension forces. Six degrees of freedom (6DoF) body motions of the platform model are measured by a HD stereo camera system. Details about the experimental setup can be found in the paper by Hu et al. (2013).

Froude scaling is used for establishing scaling factors between the model-scale and the fullscale platform. The Froude number is defined as follows:

$$Fr = U/\sqrt{gL} \tag{1}$$

where U is the characteristic velocity, and L is the corresponding characteristic length. Here we define a geometric scaling ratio by:

$$\lambda = L_{\mathrm{FS}}/L_{\mathrm{MS}} \tag{2}$$

where the subscript FS means the full scale, and the subscript MS means the model scale. The scale ratios for the commonly used variables are shown in Table 1.

Figure 3 shows the experimental setup, in which a floating wind turbine model is moored in front of the wind generator. Three wind turbines are approximated by three drag plates. The dimensions of the drag plate and the spring constant of the mooring lines are determined by the scale ratios shown in Table 1. The drag coefficient for the real Wind Lens turbine is obtained from a wind tunnel experiment. The equivalent spring constant for the actual mooring lines is calculated by using a catenary anchoring theory. In the experiment, tension forces of the mooring lines are measured, and the 6DoF body motions are measured by a noncontact method using two HD stereo cameras.

Variable	Dimensions	Scale ratio
Length	L	λ
Period	T	$\sqrt{\lambda}$
Velocity	L/T	$\sqrt{\lambda}$
Acceleration	L/T^2	1
Mass	M	λ^3
Force	ML/T^2	λ^3
Spring constant	M/T^2	λ^2
Wave height	L	λ

Table 1 Scale ratios using Froude scaling

CFD METHOD

The in-house research code RIAM-CMEN has been improved and extended to predict extremely nonlinear wave-body interactions and maximum wave and wind loads in harsh sea conditions. Figure 4 depicts the schematic description of the code to show its capability. The basic numerical scheme adopted by the CFD code is the CIP-based multi-phase simulation method. In the numerical simulation, violent free surface flows, strongly nonlinear wave-body interaction, and the effect of wind turbines and mooring lines are all included.

The main structure of the CFD code is shown in Fig. 5. The CFD core contains a flow solver to solve the nonlinear interaction

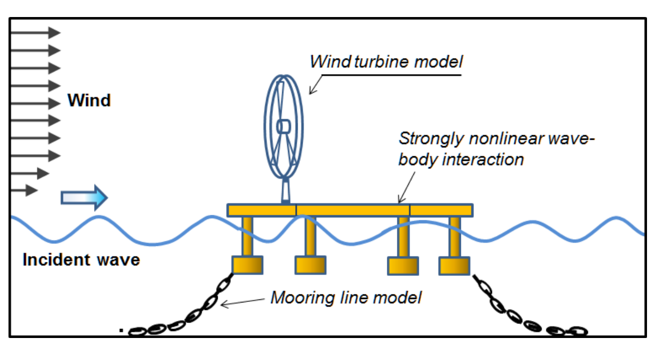

Fig. 4 Schematic description of CFD simulation

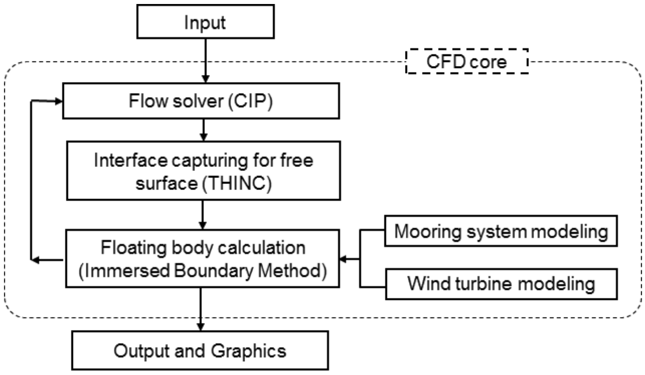

Fig. 5 Main flowchart of RIAM-CMEN

between free surface flows and the floating body, a wind turbine model to calculate wind loads on it, and a mooring line model to calculate mooring forces. The flow solver has four key features: (1) a Cartesian grid approach for wave-body interactions; (2) the CIP method (Yabe et al., 2001) as the flow solver for water and air; (3) the THINC (Tangent of Hyperbola for Interface Capturing) scheme for interface capturing of the free surface (Xiao et al., 2011); and (4) an immersed boundary method for fluid-structure interaction treatment. The CFD method has been extensively validated and applied to various kinds of marine engineering applications. Parallelization of the code and its validation have also been completed.

An extended version of RIAM-CMEN for the floating wind turbine platform has been developed, which includes the modeling of the wind turbines and mooring lines. The aerodynamic loads on the wind turbines are calculated by the actuator line model, and the mooring lines are modeled by a spring system. A detailed description of the CFD method can be found in Liu and Hu (2014).

POTENTIAL FLOW METHOD

In the potential flow method, the fluid is assumed to be inviscid, incompressible, and irrotational. The widely utilized constant panel method is used for the numerical solution. For small amplitude waves, the wave-body interaction can be modeled by a linear boundary value problem and solved by a standard boundary integral equation approach. The velocity potential on the body boundary is obtained by the following equation:

$$\frac{1}{2}\varphi(\mathrm{P})+\iint_{S_B}\varphi(\mathrm{Q})\frac{\partial G(\mathrm{P};\mathrm{Q})}{\partial \mathrm{n}}\,\mathrm{d}S=\iint_{S_B}G(\mathrm{P};\mathrm{Q})V_n\,\mathrm{d}S \tag{3}$$

where G is the free-surface Green function, and P and Q stand for the field and source point, respectively. The integral of the Rankine source term and its derivative are evaluated following the well-documented papers by Newman (1986) and Webster (1975).

Since a large number of panels will be used in the calculation of the studied platform, solving the linear algebraic system described by Eq. 3 is the most time-consuming part of the whole computation. In this study, the Generalized Minimal Residual (GMRES) method with a diagonal Jacobian preconditioner is adopted for the iterative solution, and the standard OpenMP clauses are used in the major calculation loops to accelerate the computational speed. Once the solution of Eq. 3 is found, the wave exciting force is obtained by the direct integration of the pressure on the body surface, and the hydrodynamic added mass and damping coefficient are therefore obtained by the decomposition of the radiation force.

For the aerodynamic computation of the wind turbine, the blade element momentum (BEM) theory (Glauert, 1935) is applied, which assumes that a blade can be divided into small independent elements. In this model, the axis induction factor a and tangential induction factor a' are obtained by the following equations:

$$a=\frac{1}{1+\dfrac{4F\sin^2\theta}{\sigma C_l\cos\theta+\sigma C_d\sin\theta}} \tag{4}$$

$$a'=\frac{1}{-1+\dfrac{4F\sin\theta\cos\theta}{\sigma C_l\sin\theta-\sigma C_d\cos\theta}} \tag{5}$$

where C_l and C_d are the lift and drag coefficients of the airfoil, θ is the inflow angle, and σ is the local solidity. The total loss factor F is calculated by the Prandtl model (Glauert, 1935). When $a > 0.2$, the Glauert correction is used (Spera, 1994). The Du-Selig model (Du and Selig, 2000) is adopted to include the three-dimensional effect. After the distribution of normal and tangential loads along the span of blades is solved, the total thrust force and shaft torque are integrated (Hansen, 2008) by assuming a linear variation of the load distribution between neighboring blade elements.

A quasi-static approach is used for simulating the transient motion of the floating platform. Application of the Cummins equation (Cummins, 1962) through Fourier's transformation leads to the following formula:

$$\begin{aligned}&[M_{ij}+A_{ij}(\infty)]\ddot{\xi}_j(t)+\int_0^t K_{ij}(t-\tau)\dot{\xi}_j(\tau)\,d\tau+C_{ij}\xi_j(t)\\&\quad=F_i^{\mathrm{Wave}}(t)+F_i^{\mathrm{Mooring}}(t)+F_i^{\mathrm{Wind}}(t)+F_i^{\mathrm{Viscous}}(t)\end{aligned} \tag{6}$$

where M_{ij} and C_{ij} are the mass matrix and restoring matrix of the system, respectively, K_{ij} is the retardation function, and $A_{ij}(\infty)$ is the infinite-frequency limit of the added mass. The forces on the right-hand side correspond to wave loads, mooring loads, wind loads, and viscous loads. The mooring loads are computed by a catenary theory method (Jonkman, 2007) with the consideration of the seabed friction on the mooring lines. The viscous loads are calculated by assuming that the drag force is proportional to the square of the local relative velocity, and a drag coefficient is specified at each cylindrical component. Equation 6 can be applied to both regular and irregular waves. For irregular wave problems, a prescribed wave spectrum is used. Equation 6 is numerically integrated by a fourth-order Runge-Kutta scheme.

RESULTS

Validation and improvement of the numerical methods described above are in progress. First, we need to check the accuracy of wave-body interaction prediction. For this purpose, an experiment without the consideration of wind is carried out. Numerical simulations by the proposed numerical methods are performed against the experiment, and the results are presented in this paper. Validation of the numerical methods for the case under both wind and wave conditions will be conducted in the next stage of the research.

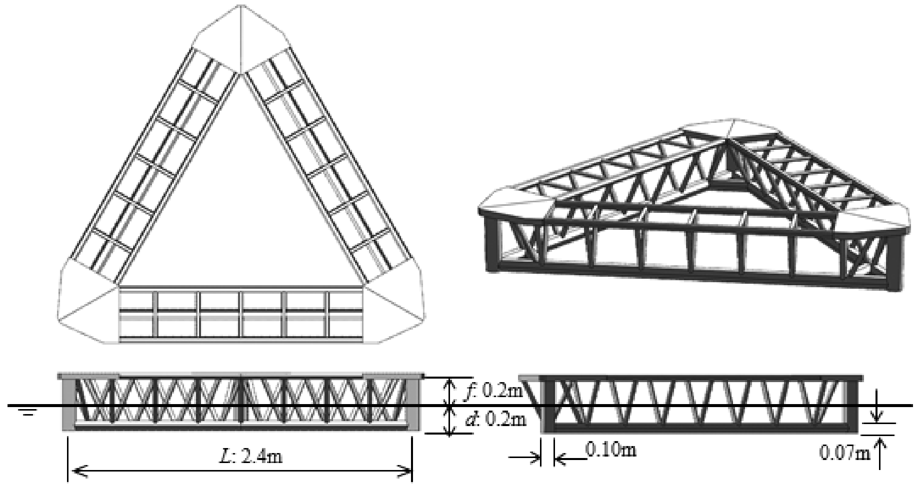

Fig. 6 Principal dimensions of the platform model

The floating platform model used in the experiment is shown in Fig. 6, which is a 1:50 scale model with the displacement of 0.01424 m^3. The incident wave angle related to the floating body is shown in Fig. 7. In the experiment, three wave height ratios ($H/\lambda = 1/50$, 1/25, 1/10) and three incident wave angles ($\beta = 0°$, 90°, 180°) are considered. Only regular waves are used.

All the numerical simulations presented below are for the incident wave angle of $\beta = 0°$. The CFD simulation is performed by using a numerical wave tank, in which a nonuniform grid with the grid number of $400 \times 280 \times 230$ in the x, y, and z directions is used with the minimum grid spaces of $\Delta x = 0.00625L$, $\Delta y = 0.005625L$, and $\Delta z = 0.00125L$. The time step size is $\Delta t/T = 1/2000$, where T is the period of the incident wave. The parallel version of RIAM-CMEN is utilized for the computation, in which 40 processors are used. The CPU time for the simulation of 30 wave periods is about 45 hours in a laboratory PC cluster system.

The results for a large wave height case ($\lambda/L = 1.3$, $H/\lambda = 1/10$) are shown in Figs. 8 and 9. In Fig. 8, the free surface variation around the floating body is compared among CFD images and experimental pictures at four time instants during one wave period T. The experimental pictures are chosen from the high-speed digital video camera record. The overall comparison of the nonlinear free surface variation around the floating platform is reasonably good. The correspondent pressure distribution on the structural surface is shown in Fig. 9. The incident wave direction is from left to

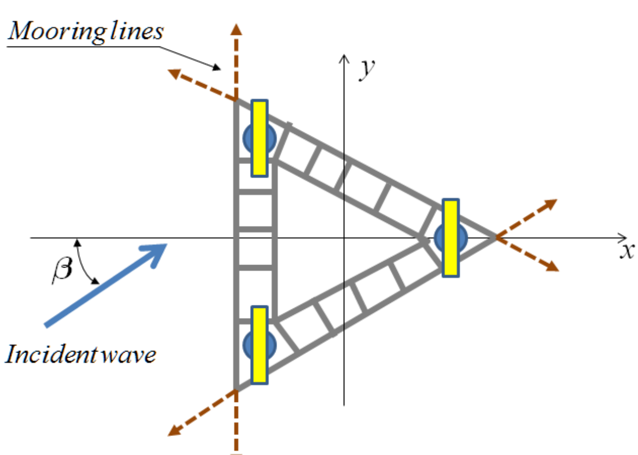

Fig. 7 Top view of the experimental setup

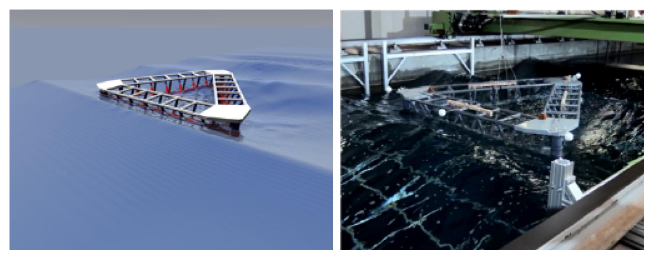

(a) $t = t_0$

(b) $t = t_0 + 0.25T$

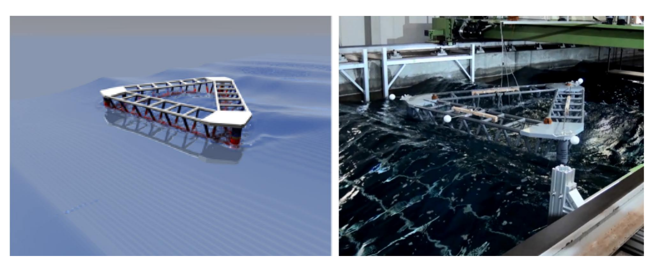

(c) $t = t_0 + 0.5T$

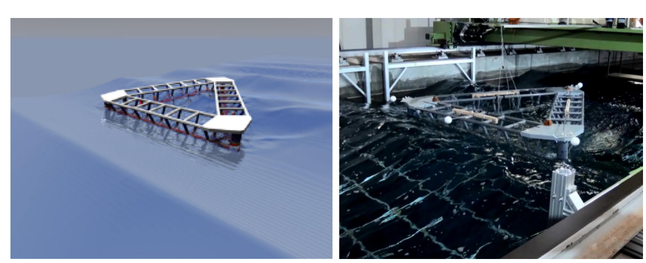

(d) $t = t_0 + 0.75T$

Fig. 8 CFD vs. experiment: free-surface profiles for the case of $\lambda/L = 1/3$ and $H/\lambda = 1/10$

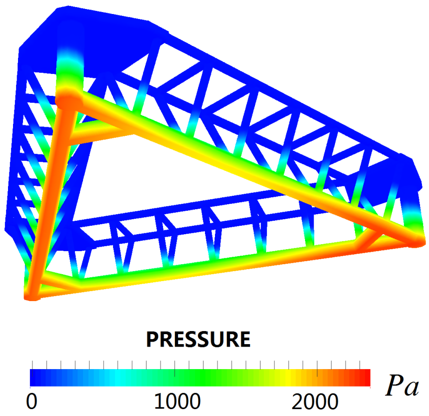

(a) $t = t_0$

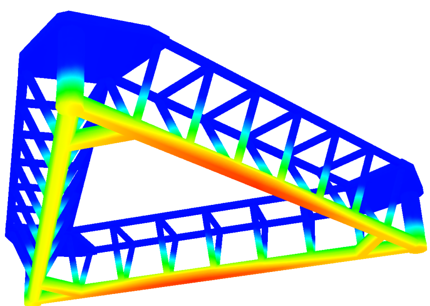

(b) $t = t_0 + 0.25T$

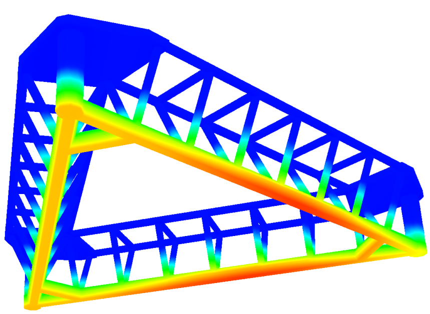

(c) $t = t_0 + 0.5T$

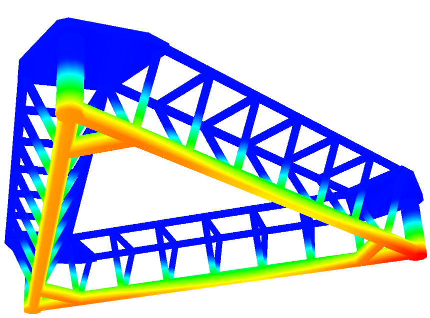

(d) $t = t_0 + 0.75T$

Fig. 9 Computed pressure distribution for the case of $\lambda/L = 1/3$ and $H/\lambda = 1/10$

right. It is demonstrated that the proposed CFD model can be a useful tool for the accurate prediction of pressure distribution, which is important information for the structural analysis of the platform.

The potential flow method is applicable to the prediction of linear wave-body interactions. Since the computation is very fast, this method can be used for parametric study. Figure 10

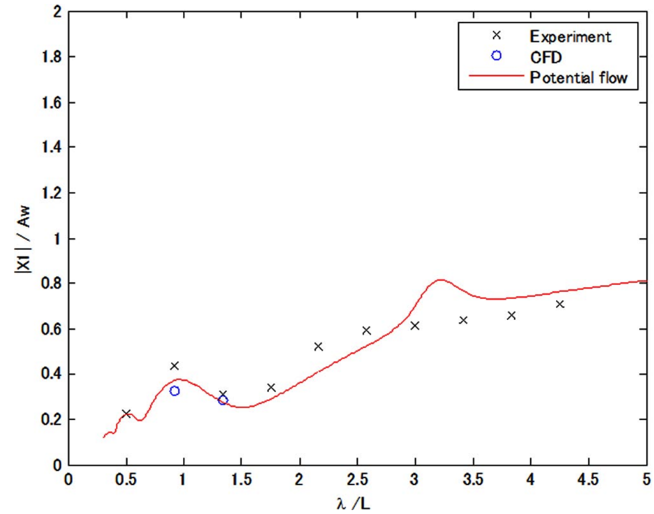

(a) Surge motion

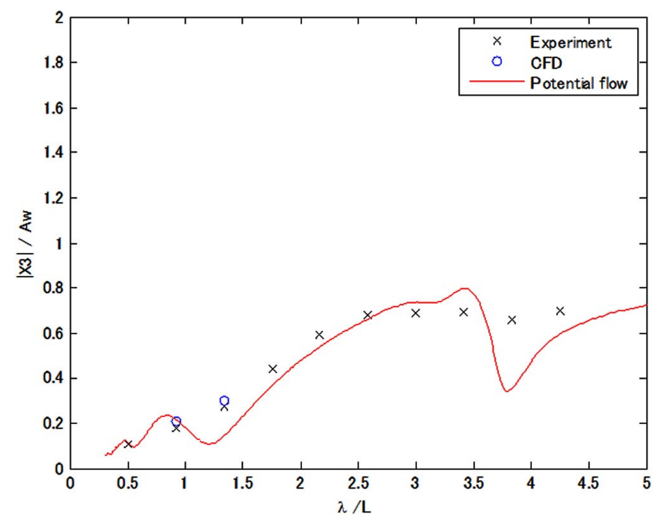

(b) Heave motion

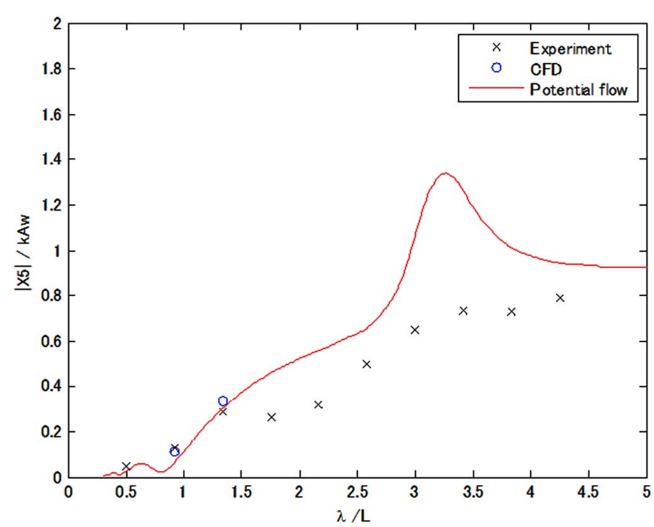

(c) Pitch motion

Fig. 10 Comparison of RAOs for $\beta = 0°$

shows the computed RAOs for $\beta = 0°$ and compares experimental measurements with CFD results. In this figure, Aw means wave amplitude. The CFD simulation is carried out on two wavelengths

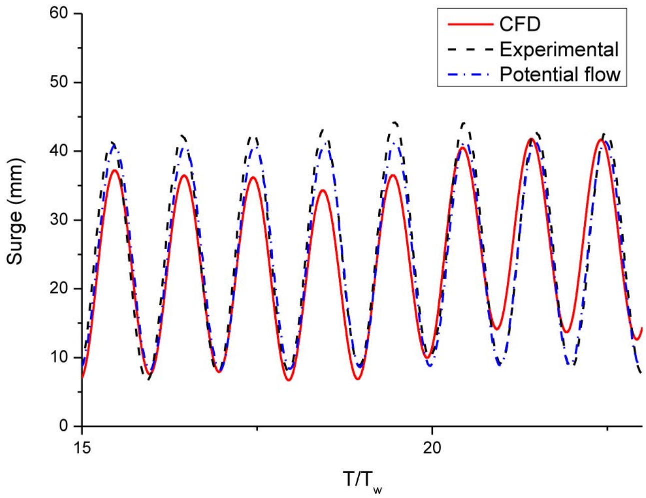

(a) Surge motion

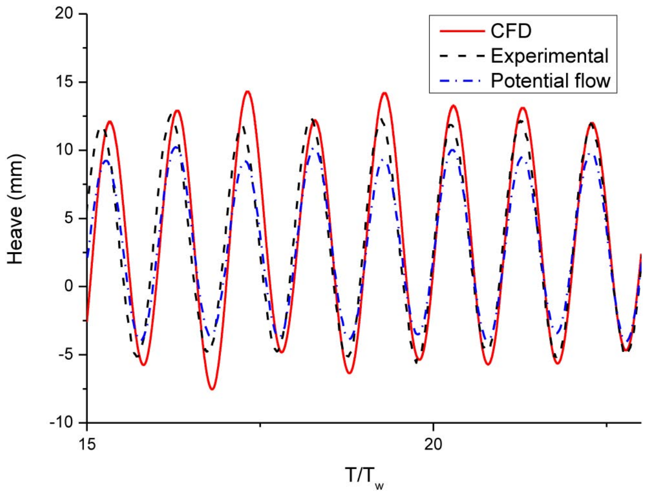

(b) Heave motion

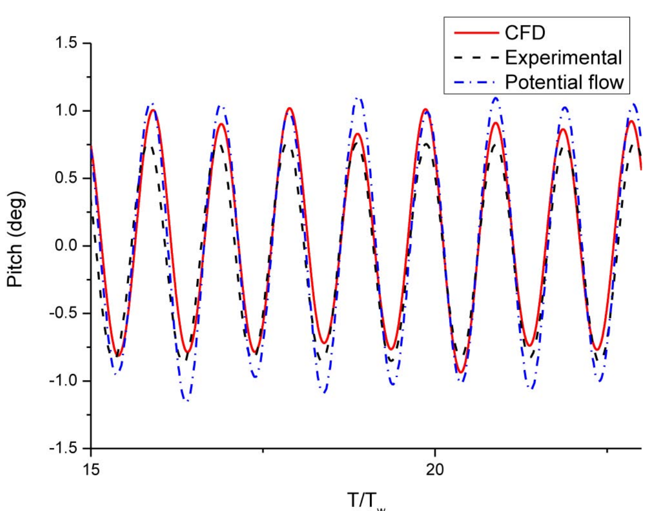

(c) Pitch motion

Fig. 11 Comparison of time history between two numerical methods and experiment for $\lambda/L = 0.9$

with small wave heights ($H/\lambda = 1/25$). The RAOs are obtained by integrating the time series over 20 wave periods. The comparison between the two methods and the experiment on RAOs is reasonably good. Disagreement between the potential flow results and the experiment is partly due to the nonlinear effect.

In Fig. 11, time histories of the body motions for the case of $\lambda/L = 0.9$ are compared among the two numerical methods and the experiment. Nonlinear features are seen for the CFD results, which can also be found in the experiment. Linear behaviors are shown for the potential flow results. Therefore, discrepancy is found by direct comparison between the CFD and the potential flow method.

CONCLUSIONS

The design of a floating offshore wind turbine system is still a big challenge due to the strict cost-effective requirements. A systematic research process is being developed in our research group for this purpose. In this study, a hydrodynamic analysis of a new floating wind turbine platform has been carried out by means of a physical experiment and two kinds of numerical methods. The potential flow method is suitable for parametric study and irregular wave response analysis. On the other hand, CFD simulation can be used to study the nonlinear phenomena in large amplitude wave conditions. The experiment is carried out in a towing tank with a movable seafloor frame and a wind generator that are newly installed 1:50 scale models are tested in the experiment, and Froude scaling is used to determine the experimental conditions. To check the calculation accuracy of the wave-body interaction, numerical simulations are performed by the proposed CFD and potential flow methods. A generally good comparison between the computations and the measurements is obtained for motions for the experimental cases.

ACKNOWLEDGEMENTS

This research is supported in part by Grants-in-Aid for Scientific Research (B), MEXT (No. 24360358). We would like to thank ClassNK (Nippon Kaiji Kyoukai), Oshima Shipbuilding Co. Ltd., Shin Kurushima Dockyard Co. Ltd., and Tsuneishi Holdings Corp. for funding this study and for permission to publish this paper.

REFERENCES

Cummins, WE (1962). “The Impulse Function and Ship Motions,” *Schiffstechnik*, 9, 101–109.

Du, Z, and Selig, MS (2000). “The Effect of Rotation on the Boundary Layer of a Wind Turbine Blade,” *Renewable Energy*, 20, 167–181.

Glauert, H (1935). “Airplane Propellers,” in *Aerodynamic Theory*, W.F. Durand (Ed), Springer Berlin, Division L, 4, 169–360.

Hansen, MOL (2008). *Aerodynamics of Wind Turbines,* Earthscan Press, 192 pp.

Hu, CH, and Kashiwagi, M (2004). “A CIP-based Method for Numerical Simulation of Violent Free Surface Flows,” *J Mar Sci Technol*, 6, 143–157.

Hu, CH, Liu, C, and Kashiwagi, M (2012). “Parallel Simulation of RIAM-CMEN for Strongly Nonlinear Wave-Ship Interaction,” *Proc 2nd Int Conf Violent Flows*, Nantes, France, 112–117.

Hu, C, Sueyoshi, M, Liu, C, Kyozuka, Y, and Ohya, Y (2013). “Numerical and Experimental Study on a Floating Platform for Offshore Renewable Energy,” *Proc 32nd Int Conf Ocean Offshore Arct Eng (OMAE 2013)*, Nantes, France, V008T09A069, doi:10.1115/OMAE2013-11133.

Jonkman, JM (2007). *Dynamics Modeling and Loads Analysis of an Offshore Floating Wind Turbine*, Technical Report NREL/EL-

500-41958, National Renewable Energy Laboratory, Golden, CO, USA.

Newman, JN (1986). "Distributions of Sources and Normal Dipoles Over a Quadrilateral Panel," *J Eng Math*, 20, 113–126.

Liu, C, and Hu, C (2014). "CFD Simulation of a Floating Wind Turbine Platform in Rough Sea Conditions," *Proc 24th Int Ocean Polar Eng Conf*, Busan, Korea, ISOPE, 1, 325–329

Spera, DA (1994). *Wind Turbine Technology*, ASME Press, 638 pp.

Webster, WC (1975). "The Flow About Arbitrary Three-dimensional Smooth Bodies," *J Ship Res*, 19(4), 206–218.

Xiao, F, Satoshi, I, and Chen, CG (2011). "Revisit to the THINC Scheme: A Simple Algebraic VOF Algorithm," *J Comput Phys*, 230, 7089–7092.

Yabe, T, Xiao, F, and Utsumi, T (2001). "The Constraint Interpolation Profile Method for Multiphase Analysis," *J Comput Phys*, 169, 556–593.